Available at
http://pvamu.edu/aam
Appl. Appl. Math.
ISSN: 1932-9466

Applications and Applied Mathematics:
An International Journal
(AAM)

Vol. 13, Issue 2 (December 2018), pp. 1157 - 1170

Study of Transport of Nanoparticles with *K-L* Model Through a Stenosed Microvessels

[1]Rekha Bali and [2]Nivedita Gupta

Department of Mathematics
Harcourt Butler Technical University
208002 Kanpur, India
[1]dr.rekhabali@rediffmail.com; [2]niveditagupta48@gmail.com

Received: June 6, 2017; Accepted: May 25, 2018

Abstract

This paper studies a constitutive equation for blood with the transport of nanoparticles in a stenosed microvessel. The flow of blood through a bell-shaped stenosed micro blood vessel has been investigated with an importance of permeable walls that treats blood as non-Newtonian fluid by using *K-L* model. This model is more appropriate than other non-Newtonian models because *K-L* model involve three parameters such as plasma viscosity, yield stress and one other chemical variable while casson model involves only one parameter i.e. yield stress. In the present paper, the effective longitudinal diffusion of nanoparticles has been studied in stenosed blood vessel considering the contribution of molecular and convective diffusion based on Taylor's theory. Also we analyze the flow characteristics of blood such as velocity, flow rate and effective diffusion during a nanoparticle assisted drug delivery process through a stenosed permeable microvessel. An explicit expression has been derived for velocity, flow rate and effective diffusion of nanoparticles depending non-linearly on rheological parameter, stenosis height and plasma viscosity. It has been shown that for a given values of rheological parameter, stenosis height and plasma viscosity, fluid velocity is maximum at the central axis and flow rate is minimum at the axis of symmetry. Also it has concluded that the effective diffusion of nanoparticles is maximum at the vessel walls and minimum at the axis of symmetry.

Keywords: *K-L* model; nanoparticles; microvessels; flow characteristics

MSC 2010 No.: 76Z05, 76R50

1. Introduction

Nanoparticles hold significant promise as a means of next generation of medicine that allows for the intravascular delivery of drugs with contrast agents. Nanoparticles assisted drug

delivery provides a mechanism for solving the problems associated with conventional drug delivery systems. To improve the delivery efficiency of nanoparticles, it is very important to study their transport in microvessels and deposition in blood flow. The transport of nanoparticles in microvesels is of great importance in several fields from chemical to environmental and biomedical engineering. Nanoparticles are nanometer sized particles and typically made of metals, oxides, carbides or carbon nanotubes. Due to the small size of nanoparticles, the dynamic delivery process, the complex vascular environment and computational fluid particle dynamics, it is very challenging to explore these phenomena in blood vessels. Spherical particles larger than 200 nm can be easily filtered by the liver and particles smaller than 10nm can be quickly filtered by kidney. Thus, particles with diameters of 10-200 nm are the ideal drug carriers in vascular circulatory system. The properties of nanoparticles such as size, shape and surface chemistry play an important role in their transport and deposition.

Blood is a complex fluid made up of components such as erythrocytes, monocytes, platelets, proteins, fibers etc. In small channels, blood represents the two-phase nature, one is peripheral layer of plasma and other is a core region of suspension of erythrocytes. This peripheral layer shows Newtonian nature and core region shows non-Newtonian nature of fluid (Bugliorello and Sevilla, 1970; Cokelet, 1972). The study of blood flow of non-Newtonian fluids with the longitudinal transport of nanoparticles in a stenosed microvessls is very interesting topic because of the fact that the number of cardiovascular diseases such as heart attacks, strokes, ischemia, angina pectoris, atherosclerosis are the leading cause of deaths. At different locations of the cardiovascular system, the unnatural and abnormal growth in the microvessels walls termed as stenosis. In cardiac related problems, the effected blood vessels get harden as an accumulation of fatty substances in inner walls. In drug delivery, the nanoparticles must reach the sites of diseases via convective and diffusive transport within the microvessels. To reach the target diseased site, nanoparticles have to marginate towards the vascular wall. Though increase in their concentration increases the number of nanoparticles being delivered. At the target site, the concentration of nanoparticles should be high enough to kill the diseased cells. Thus the study of nanoparticle distribution is important in evaluating therapeutic efficacy and considers to be the top priority in nanoparticle drug delivery modeling (Sanhai et al. 2008; Almeida et al. 2011).

Sharp (1993) derived explicit expressions for effective longitudinal diffusion considering non-Newtonian fluids with different rheological laws such as for a casson, bingham plastic and power-law fluid. Decuzzi et al. (2006) revisited the Taylor and Aris theory (1953) to derive the effective longitudinal diffusion for a Newtonian fluid. Tan et al. (2012) studied the influence of red blood cells on nanoparticles transport and dispersion. Later, Gentile (2008 and 2010), studied the longitudinal transport of nanoparticles in terms of effective diffusivity with an emphasis on the permeability of the capillary and the rheology of blood. Shaw et al. (2014) contribute to the fundamental understanding and knowledge of how the particulate nature of blood influences nanoparticle delivery. They provide new insights on the design of nanoparticles for drug carriers in nanomedicine.

Many authors have studied the blood flow in stenosed blood vessels by using non-Newtonian fluid models such as power law fluid, herschel-bulkley fluid, casson fluid, couple stress fluid, carreau-yasuda fluid cited in Chaturani (1985 and 1986); Misra (2006). Kuang and Luo (1992) proposed an equation of blood flow having three parameters such as yield stress, plasma viscosity and one other chemical variable named as *K-L* model. They suggested that *K-L* model is one of the best model for blood flow in human. Ashrafizaadeh et al. (2009)

introduced *K-L* model for lattice Boltzmann blood flow simulation. Later, Sriyab (2014) studied the blood flow characteristics such as flow rate, skin friction and resistance to blood flow in narrow arteries with bell-shaped mild stenosis by using *K-L* model.

The main purpose of the present work is to study the longitudinal transport of nanoparticles injected into the blood stream in terms of effective diffusivity with the importance of permeability of stenosed microvessel walls and the rheology of blood. In our work, a mathematical model is developed to analyze the blood flow in microvessel at low shear rate with mild bell-shaped stenosis. Blood is treated as non-Newtonian *K-L* model. The effects of rheological parameter, plasma viscosity, yield stress, permeability of microvessel and radius of the nanoparticles on effective longitudinal diffusion of the nanoparticles are analyzed in the present study.

2. Formulation of the problem

Consider a cylindrical polar coordinate system (r', θ', z') where r' and z' are along the radius of a microvessel and along the length of a microvessel respectively and θ' represents the circumferential direction. Also we consider the steady laminar flow and non-Newtonian incompressible viscous fluid described by *K-L* model flowing in the z' axial direction through a circular microvessel. The microvessel walls are permeable to the fluid and assumed to be rigid for the solute (nanoparticles). Due to permeability, fluid flow laterally across the vessel fenestration. The bell-shaped mild stenosis in microvessel is studied and the geometry of segment of microvessel with mild bell-shaped stenosis is shown in figure 1 and is defined as follows:

$$R'(z') = R_0\left(1 - ae^{-bz'^2}\right), \tag{1}$$

where $R'(z')$, R_0 are the radius of microvessel with and without stenosis respectively; a and b are non dimensional parameters defined as $a = \frac{\delta}{R_0}$, $b = \frac{m^2}{{L_0}'^2}$; δ is the stenosis height, m represents the shape of stenosis and $2{L_0}'$ is the length of stenosis in microvessel.

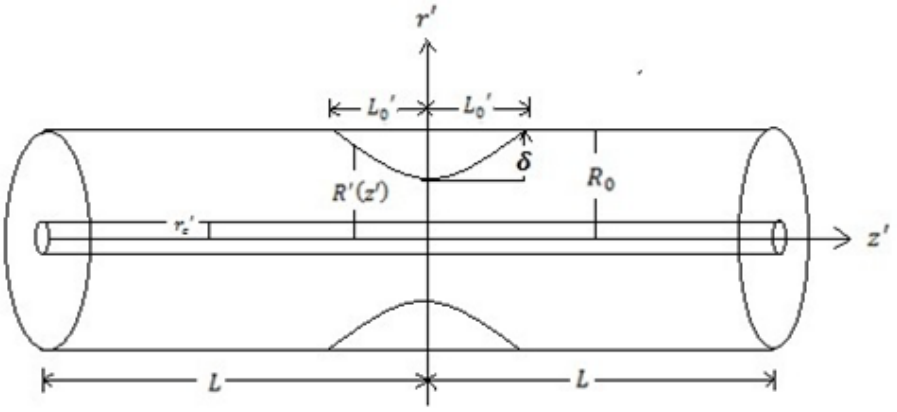

Figure 1. The transport of nanoparticles in a stenosed microvessel

Since the blood flow in microvessels is slow and steady, so magnitude and inertial forces are negligible and only one component of velocity parallel to the axis. The equation of continuity and equation of motion are given by

$$u' = u'(r')\,, \tag{2}$$

$$\frac{\partial p'}{\partial r'} = 0\ , \tag{3}$$

$$\frac{1}{r'}\frac{d}{dr'}(r'\tau') = -\frac{dp'}{dz'}\,, \tag{4}$$

p' is the pressure, ρ is the density of the fluid, u_0 is the blood velocity and L is the length of microvessel.

The constitutive equation for K-L model is defined as follows:

$$\begin{aligned} &\tau' = {\tau_y}' + \eta_2\dot{\Upsilon}^{1/2} + \eta_1\dot{\Upsilon}\,, \quad && \tau' > {\tau_y}'\,, \\ &\dot{\Upsilon} = 0\,, && \tau' < {\tau_y}', \end{aligned} \tag{5}$$

where ${\tau_y}'$, η_1 and η_2 are functions of hematocrit, plasma viscosity and other chemical variable respectively, $\dot{\Upsilon}$ is the shear rate, τ' is the shear stress.

The velocity and volumetric flow rate [Kuang (1992)] can be expressed in terms of

$$u'(r') = \begin{cases} -\frac{R'}{{\tau_R}'}\int_{\tau'}^{{\tau_R}'} f(\tau')\,d\tau', & \text{if } \tau' > {\tau_y}', \\ -\frac{R'}{{\tau_R}'}\int_{{\tau_y}'}^{{\tau_R}'} f(\tau')\,d\tau', & \text{if } \tau' < {\tau_y}', \end{cases} \tag{6}$$

$$Q'(r') = \frac{\pi R^3}{{\tau_R}'^3}\int_{{\tau_y}'}^{{\tau_R}'} {\tau'}^2 f(\tau')\,d\tau'. \tag{7}$$

Here it is assumed that fluid also flows laterally across the vessel fenestration. The fluid lateral flux does not modify the velocity within the channel but reduces the mean velocity U across the permeable walls. Mass continuity for an incompressible fluid flow is given by [Decuzzi et al. (2006)]

$$\frac{\partial Q'}{\partial z'} + V_p\lambda_p = 0, \tag{8}$$

where $V_p\lambda_p$ denotes the volume flow rate along the permeable wall per unit length, V_p is the perfusing velocity which is defined as $V_p = -L_p(\pi_i - p)$, L_p is hydraulic conductivity and π_i is the interstitial fluid pressure. Fluid depends on L_p , π_i , inlet and outlet pressures p_0 and p_1 respectively when blood flows through permeable microvessel.

Non-dimensional scheme are

$$z = \frac{z'}{L}\ ,\ r = \frac{r'}{R_0}\ ,\quad u = \frac{u'}{u_0}\ ,\ R(z) = \frac{R'(z')}{R_0}\ ,\ p = \frac{p'}{\rho {u_0}^2}\ ,\ \tau = \frac{\tau'}{\rho {u_0}^2}\,.$$

3. Solution of the problem

Solve equation (4) under the boundary condition, τ is finite at $r = 0$, we have

$$\tau = \frac{R_0}{L}\frac{r}{2}\frac{dp}{dz}. \tag{9}$$

Kuang (1992) demonstrated that r_c is the core radius of cylindrical tube within $\tau < \tau_y$, r_α is a radius at which $\tau = \tau_\alpha$ and shear stress at the wall of the tube is τ_R. From equation (5), we find the most general form of K-L model in non-dimensional form

$$f(\tau) = -\frac{du}{dr} = \begin{cases} \frac{1}{\eta_1}\rho u_0 R_0\left[\sqrt{\tau+\tau_\alpha} - \sqrt{\tau_y+\tau_\alpha}\right]^2, & if\ \tau > \tau_{y,} \\ 0, & if\ \tau < \tau_{y,} \end{cases} \tag{10}$$

where $\tau_\alpha = \frac{{\eta_2}^2}{4\eta_1} - \tau_y$ is a parameter with unit of stress.

The velocity profile and flow rate of K-L model is derived as

$$u = \begin{cases} \frac{G}{4\eta_1}\frac{dp}{dz}\left[(R^2-r^2) + 2(2r_\alpha+r_c)(R-r) - \frac{8}{3}(r_c+r_\alpha)^{\frac{1}{2}}\left\{(R+r_\alpha)^{\frac{3}{2}} - (r+r_\alpha)^{\frac{3}{2}}\right\}\right], if\ r > r_c, \\ \frac{G}{4\eta_1}\frac{dp}{dz}\left[(R^2-{r_c}^2) + 2(2r_\alpha+r_c)(R-r_c) - \frac{8}{3}(r_c+r_\alpha)^{\frac{1}{2}}\left\{(R+r_\alpha)^{\frac{3}{2}} - (r_c+r_\alpha)^{\frac{3}{2}}\right\}\right], if\ r < r_c, \end{cases} \tag{11}$$

$$\begin{aligned} Q = \frac{G}{8\eta_1}\frac{dp}{dz}\Big[&(R^4-{r_c}^4) + \frac{4}{3}(2r_\alpha+r_c)(R^3-{r_c}^3) \\ &-\frac{16}{105}(r_c+r_\alpha)^{\frac{1}{2}}\Big\{35R^2(R+r_\alpha)^{\frac{3}{2}} - \{35{r_c}^2(r_c+r_\alpha)^{\frac{3}{2}} \\ &-28R(R+r_\alpha)^{\frac{5}{2}} + 28r_c(r_c+r_\alpha)^{\frac{5}{2}} + 8(R+r_\alpha)^{\frac{7}{2}} - 8(r_c+r_\alpha)^{\frac{7}{2}}\Big\}\Big], \end{aligned} \tag{12}$$

where

$$G = \frac{\rho u_0 {R_0}^2}{L}.$$

The mean velocity is derived as

$$U = \frac{Q}{\pi {R_0}^2}. \tag{13}$$

3.1. Pressure Gradient in Permeable Capillaries

Solve equation (8) by using method of power series solution under the boundary conditions $p = p_0$ at $z = -1$ and $p = p_1$ at $z = 1$, we have

$$\begin{aligned} p = C_0 + C_1 z + \Big(&-\frac{\rho u_0 L_p \lambda_p L}{\pi {R_0}^2}\frac{4\eta_1}{G}\frac{1}{D}C_0 - \frac{A}{2D}C_1 + \frac{L_p\lambda_p L}{\pi {R_0}^2 u_0}\pi_i\frac{4\eta_1}{G}\frac{1}{D}\Big)z^2 \\ &+\Big[\frac{\rho u_0 L_p\lambda_p L}{\pi {R_0}^2}\frac{4\eta_1}{G}\frac{A}{3D^2}C_0 + \Big(\frac{\rho u_0 L_p\lambda_p L}{3\pi {R_0}^2}\frac{4\eta_1}{G}\frac{1}{D} + \frac{A^2}{6D^2}\Big)C_1 - \frac{L_p\lambda_p L}{\pi {R_0}^2 u_0}\pi_i\frac{4\eta_1}{G}\frac{A}{3D^2}\Big]z^3, \end{aligned} \tag{14}$$

where

$$A = 2ab[4(1-a)^3 + 4(1-a)^2(2r_\alpha + r_c) - 8(r_c+r_\alpha)^{\frac{1}{2}}(1-a)^2(1-a+r_\alpha)^{1/2}],$$

$$D = (1-a)^4 - {r_c}^4 + \frac{4}{3}(2r_\alpha + r_c)[(1-a)^3 - {r_c}^3]$$
$$-\frac{16}{105}(r_c + r_\alpha)^{\frac{1}{2}}\left\{35(1-a)^2(1-a+r_\alpha)^{3/2} - 35{r_c}^2(r_c+r_\alpha)^{\frac{3}{2}}\right.$$
$$\left.-28(1-a)(1-a+r_\alpha)^{5/2} + 28r_c(r_c+r_\alpha)^{\frac{5}{2}} + 8(1-a+r_\alpha)^{7/2} - 8(r_c+r_\alpha)^{\frac{7}{2}}\right\},$$

$$C_0 = \frac{p_0\psi_2 + p_1\psi_1 - \psi_1\phi_2 - \psi_2\phi_1}{\xi_1\psi_2 + \xi_2\psi_1}, \qquad C_1 = \frac{p_1\xi_1 + \phi_1\xi_2 - p_0\xi_2 - \phi_2\xi_1}{\xi_1\psi_2 + \xi_2\psi_1},$$

$$\xi_1 = 1 - \frac{\rho u_0 L_p \lambda_p L}{\pi {R_0}^2}\frac{4\eta_1}{GD}\left(1 + \frac{A}{3D}\right), \qquad \xi_2 = 1 - \frac{\rho u_0 L_p \lambda_p L}{\pi {R_0}^2}\frac{4\eta_1}{GD}\left(1 - \frac{A}{3D}\right),$$

$$\phi_1 = \frac{L_p \lambda_p L}{\pi {R_0}^2 u_0}\pi_i \frac{4\eta_1}{GD}\left(1 + \frac{A}{3D}\right), \qquad \phi_2 = \frac{L_p \lambda_p L}{\pi {R_0}^2 u_0}\pi_i \frac{4\eta_1}{GD}\left(1 - \frac{A}{3D}\right),$$
$$\psi_1 = 1 + \frac{A}{2D} + \frac{A^2}{6D^2} - \frac{4}{3}\frac{\rho u_0 L_p \lambda_p L}{\pi {R_0}^2}\frac{\eta_1}{GD}, \qquad \psi_2 = 1 - \frac{A}{2D} + \frac{A^2}{6D^2} - \frac{4}{3}\frac{\rho u_0 L_p \lambda_p L}{\pi {R_0}^2}\frac{\eta_1}{GD}.$$

3.2. The Effective Longitudinal Diffusion

Taylor and Aris (1953) introduced the idea of an effective longitudinal diffusion, for which expression is followed by Sharp (1993) as

$$\frac{1}{r}\frac{\partial}{\partial r}\left(r\frac{\partial C}{\partial r}\right) = \frac{u}{D_m}\frac{\partial C}{\partial z}, \tag{15}$$

where $u(r)$ is the non-uniform axial velocity and $C(r,z)$ is the nanoparticle concentration, D_m is the molecular diffusion coefficient. $C_1(r,z)$ denotes the concentration within the core region of microvessel and $C_2(r,z)$ denotes the concentration in the cell-free layer. Boundary conditions for both regions are given as

$$C_1 = 0 \text{ at } r = 0, \quad \frac{\partial C_1}{\partial r} = 0 \text{ at } r = 0,$$

and

$$\frac{\partial C_2}{\partial r} = 0 \text{ at } r = 1, \; C_1 = C_2 \text{ at } r = r_c\,.$$

Under above boundary conditions, we solve equation (13) for C_1 and C_2.

The flux of the solute across a section is given as

$$J = \frac{1}{\pi {R_0}^2}\left[\int_0^{r_c}\left(u_c C_1 - D_m\frac{\partial C}{\partial z}\right)2\pi r dr + \int_{r_c}^{R(z)}\left(uC_2 - D_m\frac{\partial C}{\partial z}\right)2\pi r dr\right]. \tag{16}$$

The effective diffusion coefficient is readily derived as

$$D_{eff} = -J/\frac{\partial C}{\partial z} = D_m\left[R^2 - \frac{1}{{D_m}^2}\left(\frac{G}{8\eta_1}\frac{dp}{dz}\right)^2\left(\frac{{r_c}^4}{2}H^2 + 8I\right)\right], \tag{17}$$

where

$$H = \left[(R^2 - {r_c}^2) + 2(2r_\alpha + r_c)(R - r_c) - \frac{8}{3}(r_c + r_\alpha)^{\frac{1}{2}}\left\{(R+r_\alpha)^{\frac{3}{2}} - (r_c+r_\alpha)^{\frac{3}{2}}\right\}\right],$$
$$I = \frac{64}{9}(r_c + r_\alpha)\left\{\frac{3}{35}R^2(R+r_\alpha)^5 - \frac{3}{35}{r_c}^2(r_c+r_\alpha)^{\frac{7}{2}}(R+r_\alpha)^{\frac{3}{2}}\right\}$$

$$-\frac{2}{3}R^2(r_c+r_\alpha)^{\frac{1}{2}}\left\{\frac{12}{35}R^2(R+r_\alpha)^{\frac{7}{2}}-\frac{12}{35}{r_c}^2(r_c+r_\alpha)^{\frac{7}{2}}\right\}$$
$$-\frac{8}{3}(r_c+r_\alpha)^{\frac{1}{2}}\left\{\frac{R^2}{2}(R+r_\alpha)^{\frac{3}{2}}\ln R-\frac{{r_c}^2}{2}(R+r_\alpha)^{\frac{3}{2}}\ln r_c\right.$$
$$-\frac{1}{4}(R+r_\alpha)^{\frac{3}{2}}(R^2-{r_c}^2)-\frac{2}{7}R^{7/2}\ln R+\frac{2}{7}{r_c}^{7/2}\ln r_c+\frac{4}{49}\left(R^{7/2}-{r_c}^{7/2}\right)$$
$$\left.-\frac{3}{5}r_\alpha R^{5/2}\ln R+\frac{3}{5}r_\alpha {r_c}^{5/2}\ln r_c+\frac{6}{25}r_\alpha\left(R^{5/2}-{r_c}^{5/2}\right)\right\}$$
$$-\frac{8}{3}(r_c+r_\alpha)^{\frac{1}{2}}\left\{\frac{1}{2}(R+r_\alpha)^{\frac{3}{2}}(R^2-{r_c}^2)-\frac{2}{5}R(R+r_\alpha)^{\frac{5}{2}}+\frac{2}{5}r_c(r_c+r_\alpha)^{\frac{5}{2}}\right.$$
$$\left.+\frac{4}{35}(R+r_\alpha)^{\frac{7}{2}}-\frac{4}{35}(r_c+r_\alpha)^{\frac{7}{2}}\right\}.$$

4. Results and Discussions

The most important parameters for estimating the transport of nanoparticles in stenosed blood vessel are stenosis height a, plasma viscosity η_1 and rheological parameter r_c. These made a great change in flow characteristics such as velocity, volumetric flow rate and effective longitudinal diffusion. The expressions are derived for velocity u, flow rate Q and effective longitudinal diffusion D_{eff}/D_m. The expression for effective longitudinal diffusion derived in equation (17) comprises two terms: a molecular diffusion and a convective term. The second term depends on the rheology of blood expressed through r_c. The axial velocity for *K-L* fluid model are shown in Figure 2-4. Figure 2 depicts that the variation of axial velocity with radial coordinate for different values of the stenosis height. It is observed that the axial velocity decreases with increase of stenosis height.

The effect of plasma viscosity on axial velocity is shown in Figure 3. As the plasma viscosity η_1 increases, the axial velocity changes parabolically along the radius of the vessel. It is also shown that the axial velocity decreases with increase in plasma viscosity. Figure 4 depicts that the variation of axial velocity with radial coordinate for different values of rheological parameter r_c. As r_c increases i.e., the radius of core region increases, the axial velocity along radial coordinate decreases significantly. It is also shown that the velocity in core region is flat in nature. This means that the velocity profile approaches a more parabolic shape and approaches Newtonian like profile [Ashrafizaadeh et al. (2009)] with decrease of rheological parameter, plasma viscosity and the stenosis height. Also one should note that the dimensionless velocity profiles for non-Newtonian Casson-like fluid [Gentile et al. (2008)] and Herschel Bulkley fluid model [Misra et al. (2006)] are identical in nature. These numerical results are confirmed by experimental observation which states that the blood is almost Newtonian in absence of stenosis height, plasma viscosity and rheological parameter.

The variations of volumetric flow rate with axial distance are shown in Figure 5-7. From Figure 5, it is observed that the volumetric flow rate decreases with increase of stenosis height in microvessel. At a fixed value of stenosis height a, blood flow rate attains its minimum at maximum height of the stenosis. The effect of plasma viscosity on volumetric flow rate is shown in figure 6. It is shown that blood flow rate decreases significantly with increase of plasma viscosity and affected only on stenotic region of blood vessels. Figure 7 depicts that the variation of blood flow rate with axial distance for different values of rheological parameter r_c

It is observed that blood flow rate decreases with increase of r_c, and at a fixed value of r_c, blood flow rate attains its minimum at maximum height of the stenosis. Therefore, it is concluded the volumetric flow rate of blood decreases with increase of stenosis height,

plasma viscosity as well as rheological parameter. In Casson and Herschel-Bulkley fluid model, the blood flow rate also decreases with increase of stenosis height and rheological parameter. Also Sriyab (2014) was derived the similar result for non-Newtonian *K-L* fluid model. Therefore, we can say that the nature of variation in blood flow rate is similar with the case of other non- Newtonian fluid models.

The results for the effect of non-Newtonian blood behavior on effective diffusion are shown in figure 8-10. The effect of stenosis height on effective diffusion D_{eff}/D_m is shown in figure 8. It shows that the effective diffusion decreases with increase of stenosis height a and it has minimum at maximum height of the stenosis. The influence of plasma viscosity on the effective longitudinal diffusion D_{eff}/D_m is shown in figure 9, where the variation along the channel of the effective diffusivity is plotted. As η_1 increases, the reduction in effective diffusivity becomes more and more important. Figure 10 is plotted for the effect of r_c on effective diffusion in stenotic portion of the blood vessel. It is shown that the ratio D_{eff}/D_m is minimum at maximum height of the stenosis and maximum at the wall of the blood vessel. An increase in r_c leads to a reduction of the term $I(r_c)$ and thus of D_{eff}/D_m . Therefore, it is concluded that as r_c increases, the core region of the vessel with a flat velocity profile grows and thus reduce the cell-free layer. Also at fixed r_c , effective diffusion D_{eff}/D_m decrease upto reach its minimum and then increase upto reach its maximum at the wall of the blood vessel. In Decuzzi et al. (2006) and Sharp (1993), it was shown that the rheology of the blood causes a reduction of the effective diffusion who showed a steady decrease in D_{eff}/D_m with a growing r_c .

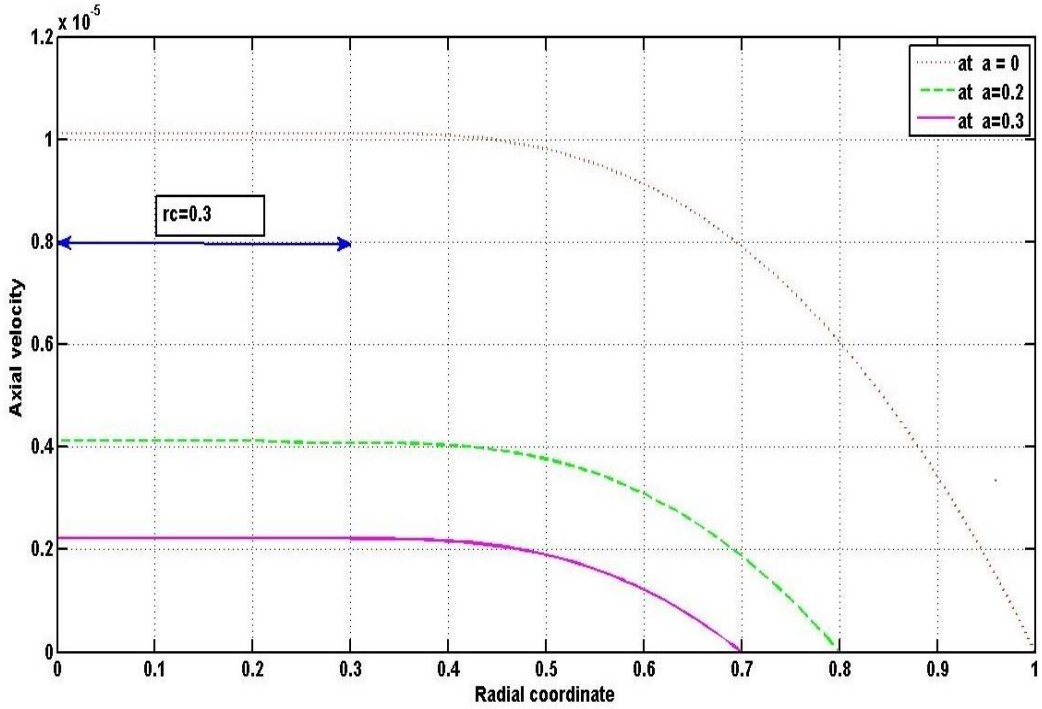

Figure 2. Variation of axial velocity with radial coordinate for different stenosis height *a*

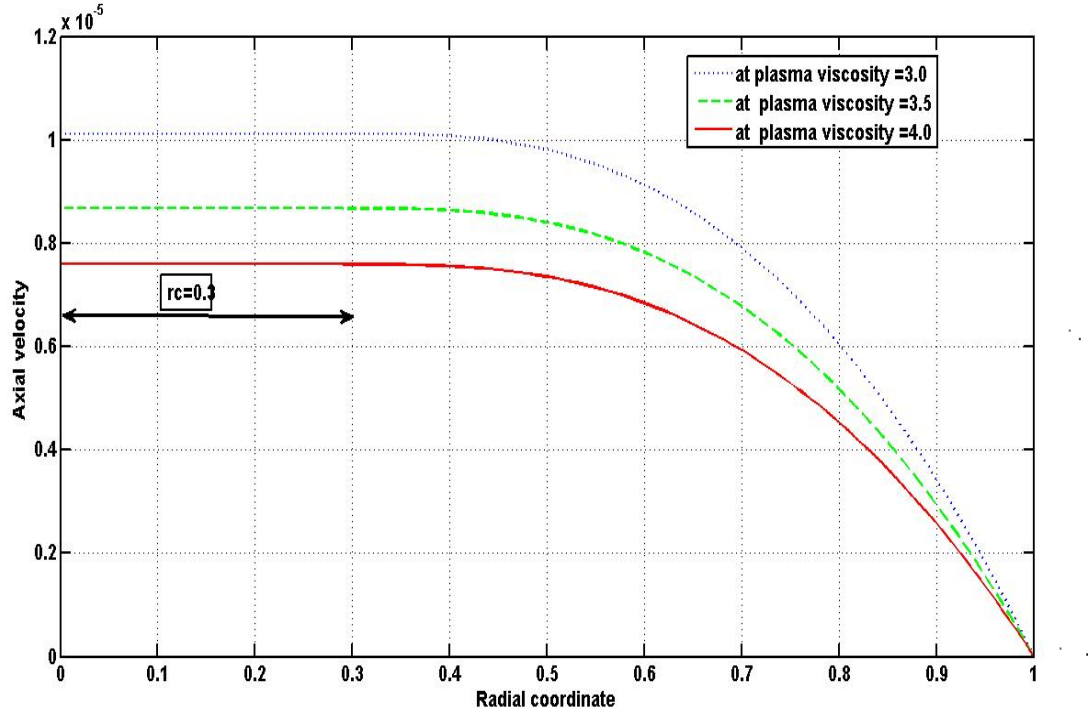

Figure 3. Variation of axial velocity with radial coordinate for different plasma viscosity η_1

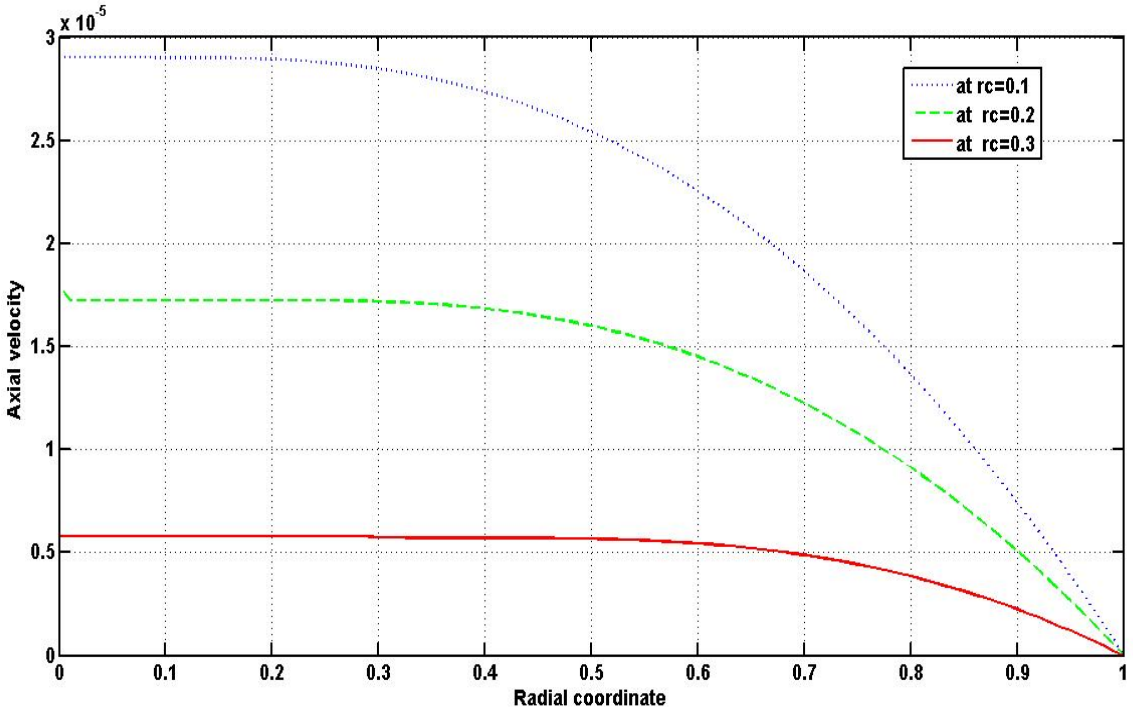

Figure 4. Variation of axial velocity with radial coordinate for different rheological parameter r_c

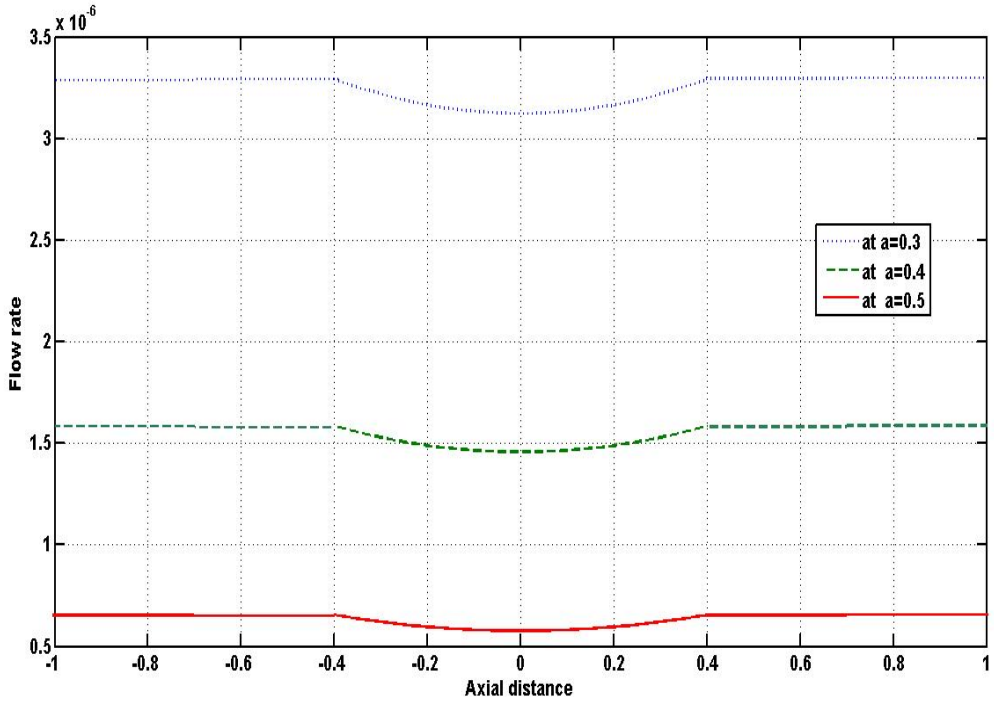

Figure 5. Variation of flow rate with axial distance for different stenosis height a

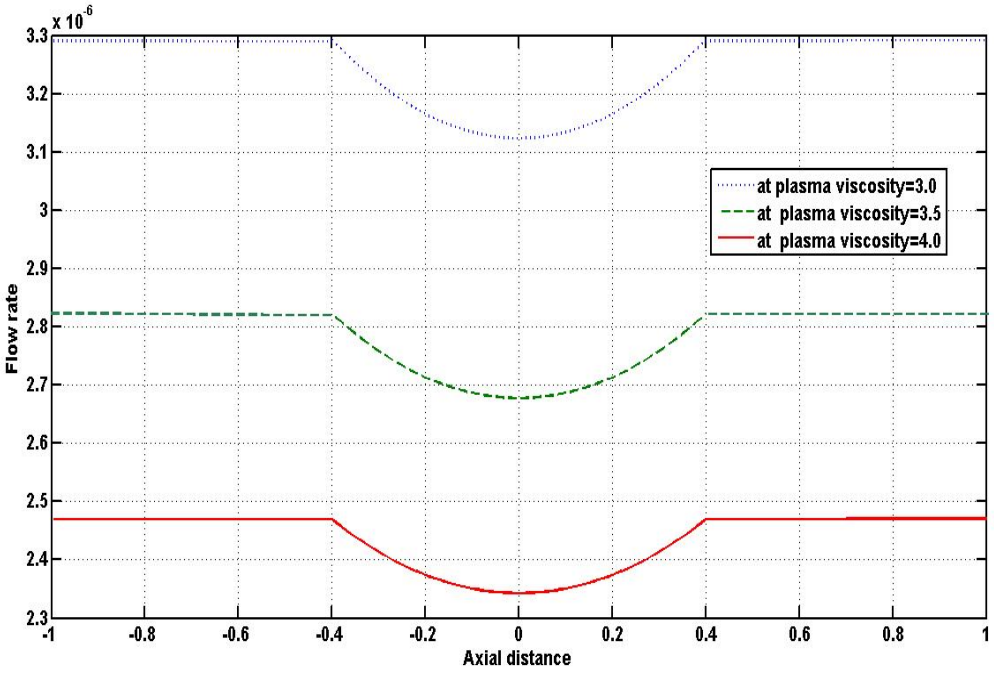

Figure 6. Variation of flow rate with axial distance for different plasma viscosity η_1

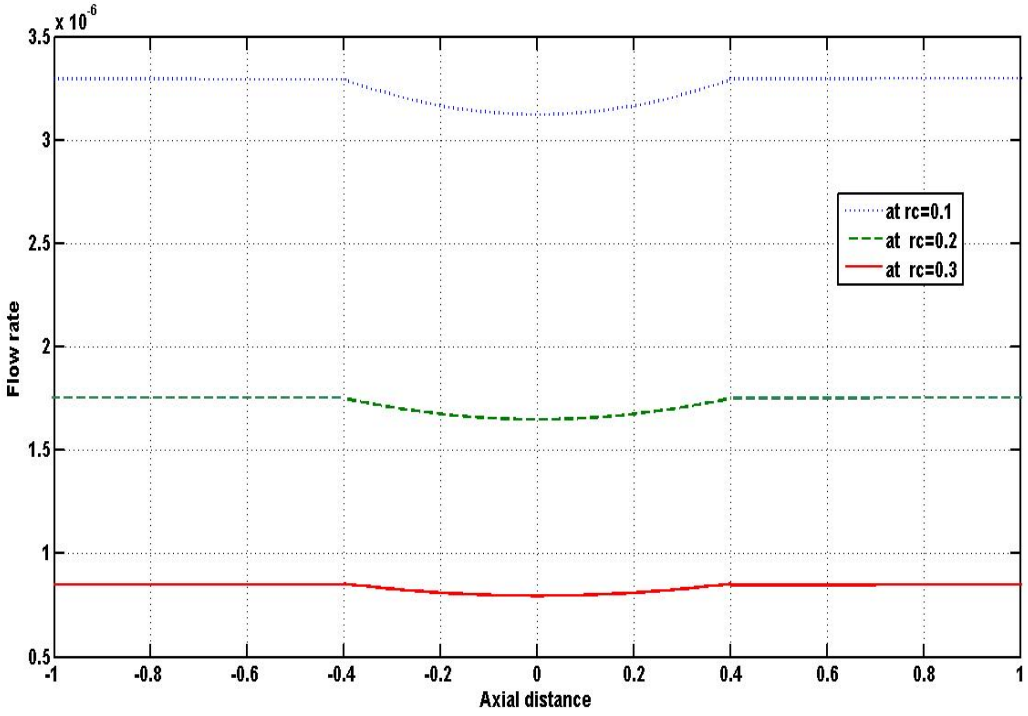

Figure 7. Variation of flow rate with axial distance for different rheological parameter r_c

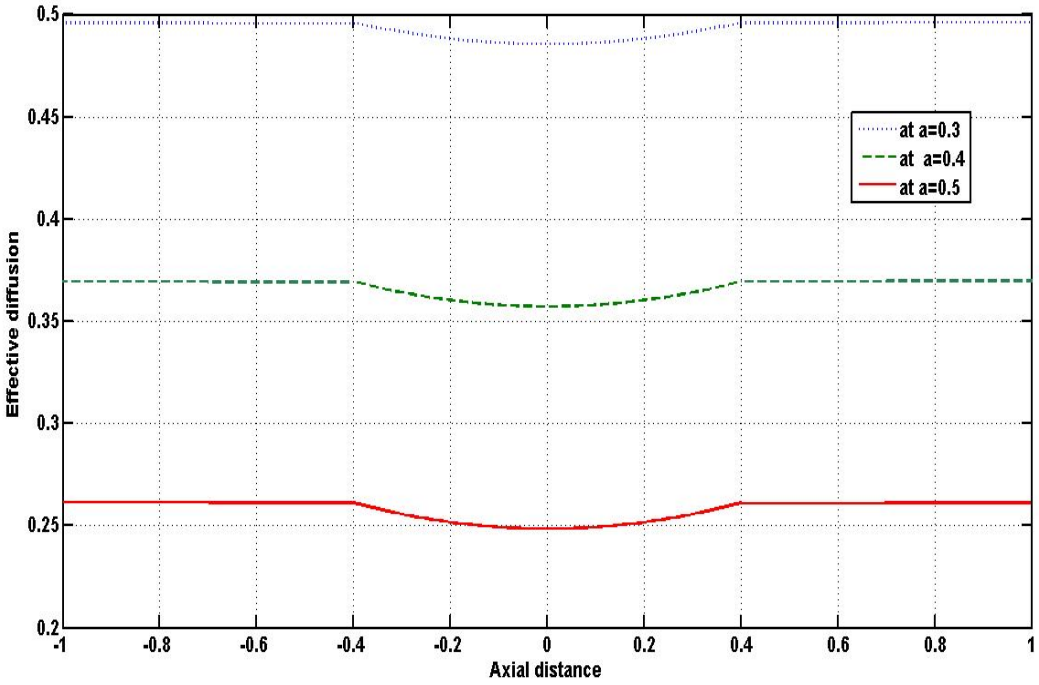

Figure 8: Variation of effective diffusion with axial distance for different stenosis height a

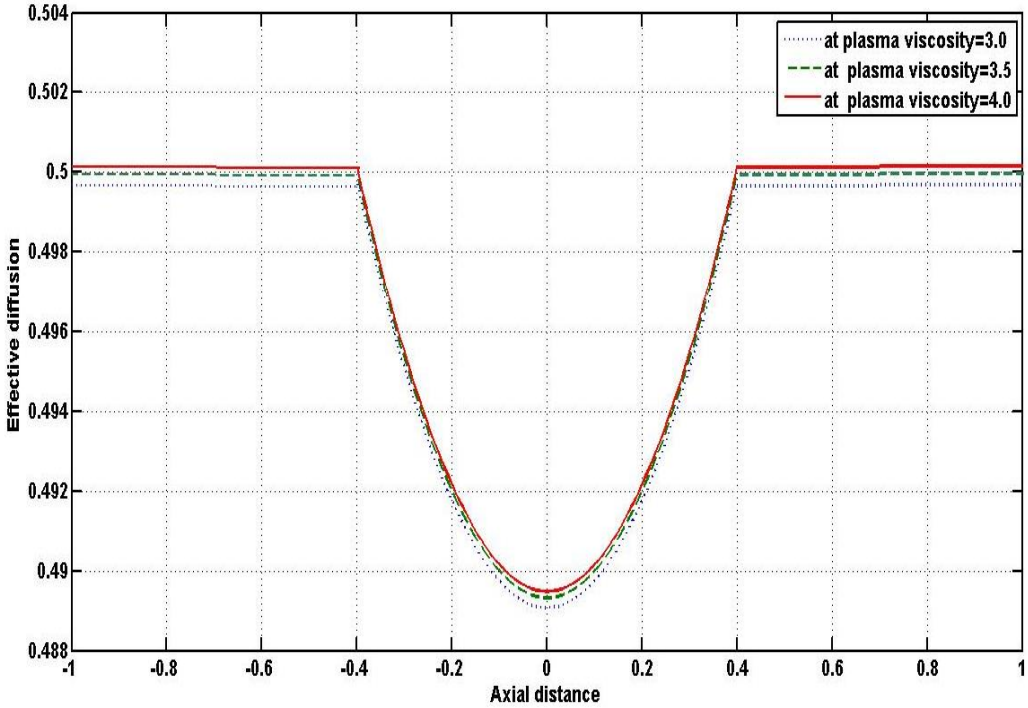

Figure 9. Variation of effective diffusion with axial distance for different plasma viscosity η_1

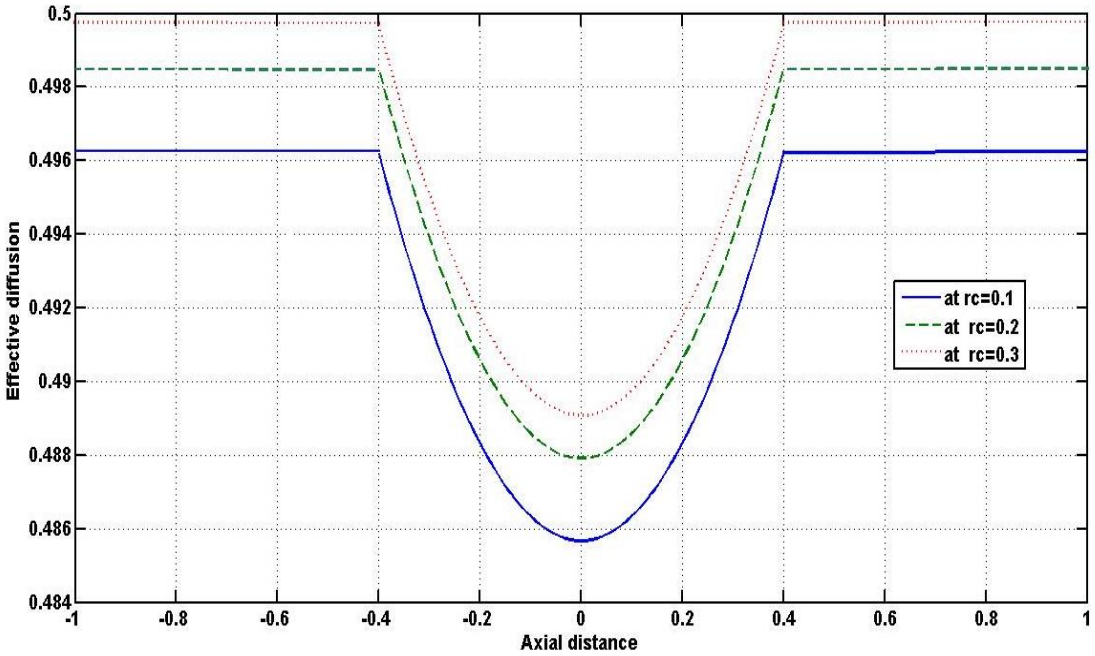

Figure 10. Variation of effective diffusion with axial distance for different rheological parameter r_c

5. Conclusions

Taylor and Aris' coefficient of diffusion has been recalled to derive the expression of effective diffusion accounting for both the diffusive and convective contribution. Taylor and Aris' approach is valid in the limit of large times or long channels i.e. in the steady state limit.

In our study, three governing parameters have been introduced namely rheological parameter r_c , plasma viscosity η_1 and stenosis height a . In the present paper, we have studied the flow characteristics of human blood during transportation of nanoparticles in a stenosed microvessel treated blood as non-Newtonian *K-L* model.

The proposed model is an improved modification of casson model because K-L model involve more parameters than casson model. Therefore, it gives more details about the flow characteristics of blood than other non-Newtonian fluid models. Analytical expressions for velocity, flow rate and longitudinal effective diffusion have been derived using appropriate boundary conditions and the computed results are presented and discussed graphically. The above study shows that the velocity is maximum at the central axis and flow rate is minimum at the axis of symmetry. Also it is observed that the effective diffusion D_{eff}/D_m depends on the stenosis height a, plasma viscosity η_1 and rheological parameter r_c . Therefore, using relevant values for r_c, η_1 and a, D_{eff}/D_m can be reduced significantly as the particle moves from larger to smaller blood vessel.

These findings provide important characteristics such as velocity, flow rate and effective diffusion that affect the transport of nanoparticles in blood vessels. A number of approaches have been taken to better understand how such characteristics of nanoparticles affect their applicability as a drug delivery system. The nanoparticles ability to target and enter tissues from blood is highly dependent on their behavior under blood flow. Therefore, this model could be used for informing new nanoparticles design and to predict general and specific uptake properties under blood flow.

REFERENCES

Almeida, J. P. M., Chen, A. L., Foster, A., Drezek, R. (2011). In vivo biodistribution of nanoparticles, Nanomedicine, 6(5), 815-835.

Aris, R. (1956). On the dispersion of a solute in a fluid flowing through a tube, Proc. R. Soc. Lond. A 235(1200), 67-77.

Ashrafizaadeh, M., Bakhsaei, H. (2009). A comparison of non-Newtonian models for lattice Boltzmann blood flow simulations, Comp. and Math. with Appl. 58, 1045-1054.

Bugliarello, G., Sevilla, J. (1970). Velocity distribution and other characteristics of steady and pulsatile blood flow in fine glass tubes, Biorheology 7, 85-107.

Chaturani, P. and Ponnalagar, Samy V. R. (1985). A study of non- Newtonian aspects of blood flow through stenosed arteries and its applications in arterial diseases, Biorheology, 22(6), pp. 521-531.

Chaturani, P., and Samy, R. P. (1986). Pulsatile flow of Casson's fluid through stenosed arteries with applications to blood flow, Biorheology, 23(5), pp. 499-511.

Cokelet, G.R. (1972). The rheology of human blood in biomechanics: its foundation and objectives, Prentice Hall. Englewood Cliffs, New Jersey. pp. 63-103.

Decuzzi, P., Causa, F., Ferrari, M., and Netti, P. A. (2006). The effective dispersion of nanovectors within the tumor microvasculature, Ann. Biomed. Eng. 34:633-641.

Gentile, F., Ferrari, M., Decuzzi, P. (2008). The transport of nanoparticles in blood vessels: the effect of vessel permeability and blood rheology, Ann Boimed. Eng. 36 (2), 254-261.

Gentile, F., Decuzzi, P. (2010). Time dependent dispersion of nanoparticles in blood vessels, J. Biomed. Sci. and Eng. 3, 517-524.

Kuang, Z.B., Luo, X.Y. (1992). A study on the constitutive equation of blood, J. Biomechanics, 25(8), 929-934.

Misra, J.C., Shit, G.C. (2006). Blood flow through arteries in a pathological state: a theoretical study, Int. J. of Engg. Sci., 44(10), 662-671.

Sanhai, W.R., Sakamoto, J. H., Canady, R., Ferrari, M. (2008). Seven challenges for nanomedicine, Nat Nano 3(5), 242-244.

Sharp, M.K. (1993). Shear-augmented dispersion in non- Newtonian fluids, Ann. Biomed. Eng. 21: 407-415.

Shaw, S., Ganguly, S., Sibanda, P., Chakraborty, S. (2014). Dispersion characteristics of blood during nanoparticle assisted drug delivery process through a permeable mirovessel, Microvasc. Res. 92, 25-33.

Sriyab, S. (2014). Mathematical Analysis of non-Newtonian blood flow in stenosis narrow arteries, Comp. and Math. Met. in med., article ID 479152.

Tan, J., Thomas, A., Liu, Y. (2012). Influence of red blood cells on nanoparticle targeted delivery in microcirculation, Soft Matter 8 (6), 1934-1946.

Taylor, G. (1953). Dispersion of soluble matter in solvent flowing slowly through a tube, Proc. R. Soc. Lond. A 219(1137):186-203.